Kinetic Analysis of F-actin Depolymerization in Polymorphonuclear Leukocyte Lysates Indicates That Chemoattractant Stimulation Increases Actin Filament Number without Altering the Filament Length Distribution

Manuel L. Cano,* Douglas A. Lauffenburger,§ and Sally H. Zigmond‡

Departments of Chemical Engineering* and Biology,‡ University of Pennsylvania, Philadelphia, Pennsylvania 19104; and Department of Chemical Engineering,§ University of Illinois at Urbana-Champaign, Urbana, Illinois 61801

Abstract. The rate of filamentous actin (F-actin) depolymerization is proportional to the number of filaments depolymerizing and changes in the rate are proportional to changes in filament number. To determine the number and length of actin filaments in polymorphonuclear leukocytes and the change in filament number and length that occurs during the increase in F-actin upon chemoattractant stimulation, the time course of cellular F-actin depolymerization in lysates of control and peptide-stimulated cells was examined. F-actin was quantified by the TRITC-labeled phalloidin staining of pelletable actin. Lysis in 1.2 M KCl and 10 μM DNase I minimized the effects of F-actin binding proteins and G-actin, respectively, on the kinetics of depolymerization. To determine filament number and length from a depolymerization time course, depolymerization kinetics must be limited by the actin monomer dissociation rate. Comparison of time courses of depolymerization in the presence (pointed ends free) or absence (barbed and pointed ends free) of cytochalasin suggested depolymerization occurred from both ends of the filament and that monomer dissociation was rate limiting. Control cells had $1.7 \pm 0.4 \times 10^5$ filaments with an average length of 0.29 ± 0.09 μm. Chemoattractant stimulation for 90 s at room temperature with 0.02 μM *N*-formylnorleucylleucylphenylalanine caused a twofold increase in F-actin and about a twofold increase in the total number of actin filaments to $4.0 \pm 0.5 \times 10^5$ filaments with an average length of 0.27 ± 0.07 μm. In both cases, most ($\sim$80%) of the filaments were quite short ($\leqslant$0.18 μm). The length distributions of actin filaments in stimulated and control cells were similar.

CHEMOATTRACTANTS induce migration of polymorphonuclear leukocytes (PMNs)[1] by stimulating formation of lamellipodia. Lamellipodia formation on cells exposed to chemoattractant occurs concomitantly with actin polymerization (Zigmond and Sullivan, 1979; Fechheimer and Zigmond, 1983; Wallace et al., 1984; Howard and Oresajo, 1984*a*,*b*; Rao and Varani, 1982). The actin polymerization is required for lamellipodia extension since cytochalasin, a drug which inhibits actin polymerization, also prevents lamellipodia extension (White et al., 1983; Cooper, 1987; Yahara et al., 1982).

The mechanism through which chemoattractant causes an increase in cellular filamentous actin (F-actin) is unclear. The increase could be accomplished by increasing the monomer globular actin (G-actin) pool available for polymerization or by increasing the effective affinity of the filament for G-actin. For example, if the high-affinity, barbed ends, of the filaments are normally blocked, the G-actin is at steady state with the low-affinity pointed end. Making free barbed ends available would increase the overall affinity of the filaments and stimulate polymerization. Free barbed ends could arise by some combination of removing capping proteins from existing filaments, cutting filaments, or creating new actin oligomers. Finally, changes in accessory proteins that alter either the association or dissociation rates at either end of the filament could shift the F-actin steady state in the cell (Lal and Korn, 1986; Broschat, 1990; Broschat et al., 1989; Weigt et al., 1990).

Insight into the mechanism through which chemoattractants regulate F-actin levels might come from knowing whether the increase in F-actin upon addition of chemoattractant results from an increase in the length and/or the number of actin filaments. It is difficult to quantify morphologically the number and lengths of actin filaments in PMNs since the F-actin is present in a cross-linked actin meshwork in which it is impossible to identify filament ends (Ryder et

1. *Abbreviations used in this paper*: CD, cytochalasin D; F-actin, filamentous actin; fNLLP, *N*-formylnorleucylleucylphenylalanine; G-actin, globular actin; PMN, polymorphonuclear leukocyte.

al., 1984). Similar F-actin meshworks have been observed in macrophages and *Dictyostelium discoideum* (Hartwig and Shevlin, 1986; Hartwig and Yin, 1988; Rubino and Small, 1987). It is possible to determine the number and length of linear polymers such as F-actin and microtubules by analyzing the time course of depolymerization (Johnson and Borisy, 1977; Karr et al., 1980; Kristofferson et al., 1980; Grazi and Trombetta, 1986; and Podolski and Steck, 1990). The relationship between G- and F-actin is described mathematically by the following equation:

$$\frac{dF}{dt} = k_{on,b} N_b [G] + k_{on,p} N_p [G] - k_{off,b} N_b - k_{off,p} N_p \quad (1)$$

where F is the total quantity of actin in filaments, $k_{on,b}$ and $k_{on,p}$ the association rate constants for the barbed and pointed ends, $k_{off,b}$ and $k_{off,p}$ the dissociation rate constants for the barbed and pointed ends, [G] the G-actin concentration, and N_b and N_p the number of barbed and pointed ends.

When the concentration of G-actin, [G], in Eq. 1 is small enough such that $(k_{off,b} + k_{off,p}) >> (k_{on,b} + k_{on,p})[G]$, Eq. 1 becomes:

$$\frac{dF}{dt} = - k_{off,b} N_b - k_{off,p} N_p \quad (2)$$

and the depolymerization rate is proportional to the number of filament ends. A change in rate then provides a measure of the change in filament number. As filaments depolymerize completely, the number of filaments decreases and therefore the depolymerization rate decreases. Since actin depolymerizes at a constant rate (length/time) the change in the filament number as a function of time is equal to the change in the filament number as a function of filament length. The depolymerization time course can thus be used to determine the number of filaments of various lengths, the filament length distribution.

We have used the kinetics of F-actin depolymerization in PMN lysates to determine the filament length distribution in PMNs. This kinetic approach required that the depolymerization rate not be limited by G-actin, filament-capping proteins, and/or filament-binding factors. We have established conditions that meet these requirements for ~70% of the F-actin, and used these conditions to examine the effect of chemoattractant stimulation on the filament length distribution.

Materials and Methods

Materials

Phalloidin, TRITC-labeled phalloidin (TRITC-phalloidin), cytochalasin D, deoxyribonuclease I (DNase I, type II, from bovine pancreas chromatographically purified), β-glycerophosphate, Hepes, ATP, NP-40, protease inhibitors (leupeptin, benzamidine, TAME-HCl, aprotonin, and PMSF) and *N*-formylnorleucylleucylphenylalanine (fNLLP) were obtained from Sigma Chemical Company (St. Louis, MO).

Cells

Rabbit peritoneal polymorphonuclear leukocytes from a 4-h exudate induced with shellfish glycogen were obtained as previously described (Zigmond and Sullivan, 1979). The cells were washed twice with saline (0.9%) and suspended in cell buffer: HBSS without Ca^{2+}, Mg^{2+}, bicarbonate, and phenol red (Gibco Laboratories, Grand Island, N.Y.) and with 10 mM Hepes, pH 7.2. Stimulated cells were incubated at room temperature with 0.02 μM of the chemoattractant fNLLP for 90 s unless otherwise stated. Control experiments showed that under these conditions the F-actin level peaks between 15 and 30 s and remains elevated and stable for ~150 s. Cells were lysed at room temperature by mixing equal volumes of cells in cell buffer with 2× lysis buffer. Lysis buffer (1× final concentrations) contained 2 mM $MgCl_2$, 5 mM EGTA, 1.2 M KCl, 1% NP-40, 2 mM KPO_4 buffer, 10 mM β-glycerophosphate, 10 mM Hepes, 5 mM ATP, and protease inhibitors (1 μg/ml leupeptin, 1 μg/ml benzamidine, 10 μg/ml TAME-HCl, and 10 μg/ml aprotonin added from a 100× stock; and 1 mM PMSF added just before lysis). When noted the lysis buffer was modified by varying KCl concentration (final KCl concentrations are given), by including 10 μM DNase I to bind G-actin, or by leaving out NP-40. Unless otherwise noted, the final cell concentration in the lysate was 2×10^6 cells/ml and each sample contained 5×10^6 total cells.

F-actin in the Cell Lysate

F-actin in the cell lysate was quantified by extending the method of Howard and Oresajo (1985*b*) using TRITC-phalloidin present at 0.6 μM. Since 10^6 cells contains ~0.13 nmole of actin (White et al., 1983), even if all of the cell actin in the lysate were polymerized (2×10^6 cells/ml = 0.26 μM), the amount of TRITC-phalloidin would be present in a 2.3-fold molar excess of the amount of F-actin. This concentration of TRITC-phalloidin stabilized F-actin and prevented depolymerization even in the presence of DNase I. Cell lysates (2×10^6 cells/ml, 5×10^6 cells/sample) were incubated for at least 60 min in TRITC-phalloidin. The samples were spun for 15 min at 80,000 rpm in the 100.3 rotor at 4°C in a TL-100 tabletop ultracentrifuge (Beckman Instruments, Inc., Palo Alto, CA) (346,000 *g*). Ultracentrifuge spins of cell lysates at 80,000 rpm for up to 60 min caused no F-actin pelleting beyond that observed with a 15-min spin. The supernatant was removed and the pellet was extracted for 24 to 48 h in 1 ml of methanol. The fluorescence was read in a fluorescence spectrophotometer (LS-5; Perkin Elmer Corp., Norwalk, CT) (excitation 540 nm/emission 575 nm). Under these conditions the TRITC staining was proportional to the amount of F-actin. Nonsaturable staining (staining in the presence of 6-μM unlabeled phalloidin; between 10 and 20% of total stain) was subtracted from all data.

G-actin in the Cell Lysate

Cells were lysed with 1 ml of lysis buffer containing 0.6 M KCl (final concentration) at 5×10^6 cells/ml. The lysate was immediately diluted 1:8 (to ~6×10^5 cells/ml) with lysis buffer without NP-40 since high concentrations of NP-40 interfered with the DNase inhibition assay. At various times, the F-actin remaining was stabilized by adding 0.6 μM TRITC-phalloidin. The samples were spun 2.5 h at 30,000 rpm (81,000 *g* in Type 40 rotor) in an ultracentrifuge (L8-80M; Beckman Instruments, Inc.). The supernatant was saved and assayed for G-actin by DNase inhibition (Blikstad et al., 1978). DNase I was stored frozen at a concentration of 1 mg/ml in 500 mM Tris-HCl (pH 7.5), 0.1 mM PMSF, and 1 mM $CaCl_2$. The DNase I was diluted 1:100 with glass-distilled water immediately before use. Calf thymus DNA (type I; Sigma Chemical Co., St. Louis, MO) was prepared in 0.1 M Tris-HCl (pH 7.5), 4 mM $MGSO_4$, and 1.8 mM $CaCl_2$ at ~200 μg/ml and diluted 1:5 before use. The activity of the DNase was determined by mixing 50 μl of the DNase solution with an appropriate volume of the supernatant between 50 and 100 μl) to cause ~50% inhibition of DNase and 1 ml of the DNA solution at room temperature. The change in optical density at 285 nm was recorded in a spectrophotometer (model 25a; Beckman Instruments, Inc.). Under these conditions, the decrease in DNase activity was shown to be proportional to the amount of G-actin present.

F-actin Quantitation on Gels

Stimulated cell lysates were processed as described in the Materials and Methods for F-actin in the cell lysate. The high speed pellets containing F-actin were analyzed by SDS-PAGE according to the methods of Laemmli (1970). The gels were stained with Coomassie blue. Actin bands on the gels were quantified with an Image One image analysis system (Universal Imaging Corporation, West Chester, PA).

Determination of Actin Association and Dissociation Rate Constants

Pyrene actin polymerization and depolymerization were used to measure actin association and dissociation rate constants under our conditions. Pyrene-labeled rabbit skeletal muscle actin was prepared as previously de-

scribed (Spudich and Watt, 1971; Northrop et al., 1986; Carson et al., 1986). Pyrene actin (2.0 μM) was polymerized overnight in 0.14 M KCl, 2 mM $MgCl_2$, 1 mM ATP, 25 mM Tris-HCl (pH 7.4), 1 mM EGTA, and 0.2% NP-40. To estimate rate constants from polymerization and depolymerization time courses, the filament number must be known. To determine the filament number present in our assay, a standard curve of elongation rate as a function of filament number was developed using villin-nucleated pyrene actin filaments as follows: Pyrene actin (2.0 μM) was polymerized overnight in the presence of 20 nM villin in 2 mM $MgCl_2$, 0.14 M KCl, 10 mM Tris-HCl (pH 7.4), 1 mM ATP, and 0.2 mM $CaCl_2$ to make villin-capped actin filaments. The concentration of filaments was taken to be equal to the concentration of villin (Northrop et al., 1986). Aliquots (10–50 μl) of villin-capped actin filaments were added to lysis buffer containing 0.15 M KCl with 1.0 μM pyrene G-actin. Since lysis buffer contains EGTA, the villin cap comes off of the filaments and the pyrene G-actin polymerizes rapidly on the free barbed ends. The initial fluorescence increase (excitation 370/emission 410), the initial elongation rate, was measured for different filament numbers added. This standard curve was then used to determine the number of filaments created when 50 μl of previously polymerized 2.0 μM pyrene actin is added (with a 50-μl Hamilton syringe) to 1 ml of lysis buffer containing 0.15 M KCl and 1.0 μM pyrene G-actin. The initial elongation rate is proportional to the number of filaments added.

The dissociation rate constant (barbed and pointed ends together) was measured by using a 50 μl Hamilton syringe to dilute 2.0 μM of previously polymerized pyrene actin to 0.1 μM in 1 ml of lysis buffer containing 0.15 M KCl without DNase I. The initial slope of the decrease in pyrene fluorescence (excitation 370/emission 410) and the filament concentration (determined from the standard curve) were used to estimate the dissociation rate constant in this buffer. By comparing the depolymerization of equal numbers of pyrene-labeled actin filaments in lysis buffer containing 0.15 or 1.2 M KCl, the actin dissociation rate constant in lysis buffer containing 1.2 M KCl was estimated. Since the dissociation rate constant in 0.15 M KCl was 2.5 s^{-1} for the barbed and pointed ends together, and the depolymerization rate increased by 1.7-fold because of the presence of 1.2 M KCl, the dissociation rate constant from both ends together in lysis buffer containing 1.2 M KCl was 4.2 s^{-1}. The presence of 1.2 M KCl and 10 μM DNase I increased this rate an additional 1.5-fold, so the dissociation rate constant under our experimental lysis conditions was 6.3 s^{-1}. Control experiments showed that DNase I did not sever F-actin because it increased the depolymerization rate by the same amount for long and short filaments. Severing would result in a greater increase in depolymerization rate for longer filaments.

The association rate constant (barbed and pointed ends together) was measured by using a 50 μl Hamilton syringe to add 50 μl of previously polymerized 2.0 μM pyrene actin to 1 ml of lysis buffer containing 0.6 M KCl and 2.0 μM pyrene G-actin. The initial slope of the increase in pyrene fluorescence (excitation 370/emission 410) and the filament concentration (determined from the standard curve) were used to estimate the association rate constant in this buffer. Therefore, under the conditions used for the elongation experiments (0.6 M KCl), the association rate constant was 0.9 μM^{-1} s^{-1}.

Assay for Number of Elongation Sites

The number of filament-barbed ends in cell lysates was estimated independently by following their ability to nucleate pyrene actin polymerization in a cytochalasin sensitive manner. Assays were performed as described previously (Carson et al., 1986) with the following modifications. Cells were lysed with lysis buffer containing 0.6 M KCl at 10^6 cells/ml in a 1-ml cuvette. At various times after lysis, a final concentration of 2.0 μM pyrene actin was added to the sample from a stock solution of 8–15 μM. The initial rate of fluorescence increase at room temperature was measured and used as an indicator of the relative number of actin elongation sites present. The absolute number was calculated by converting the change in fluorescence into a change in concentration of F-actin and using the association rate constant, 0.9 μM^{-1} s^{-1}, measured under these conditions (see above).

Results

The Cell F-actin Depolymerization Time Course Can be Followed by Decreases in the Pelletable TRITC-Phalloidin

In preliminary experiments, we found that after lysis in buffer containing 0.15 M KCl and 10 μM DNase I (to bind up G-actin), only ~30% of the cell F-actin depolymerized in 5 min and only ~50% depolymerized even after 18 h. This concentration of DNase was ~100-fold in excess of the G-actin concentration which we estimate to be ~0.1 μM in the lysate (as measured by DNase inhibition); thus the presence of G-actin was not likely to be limiting depolymerization. Increasing the KCl to 0.6 and 1.2 M KCl allowed a larger fraction of the cellular F-actin to depolymerize, 50 and 70% in 5 min, respectively. Since we wanted to analyze as large a fraction of the cellular F-actin as possible, we performed subsequent experiments in high KCl.

Cells were lysed in buffer containing 0.6 M KCl and 10 μM DNase I; at various times TRITC-phalloidin was added to stop further depolymerization and to stain the F-actin present. The F-actin was pelleted at high speed and the TRITC-phalloidin extracted from the pellet served as a measure of the F-actin. As seen in Fig. 1 *a* there was a rapid phase of F-actin loss in which ~50% of the pelletable TRITC-phalloidin was lost in two minutes and a slow phase in which an additional 30% of the TRITC-phalloidin was lost over the subsequent 18 h.

The validity of the TRITC-phalloidin pelleting assay for F-actin was confirmed by measuring the G-actin released into the supernatant with a DNase inhibition assay (Blikstad et al., 1978). This depolymerization time course was obtained by lysing cells at high dilution (~6×10^5 cells/ml) since we could not use DNase I in this experiment to lower the G-actin concentration. Fig. 1 *b* shows the increases in G-actin over time for cells lysed in buffer containing 0.6 M KCl. A rapid increase in G-actin during the first two minutes was followed by a more gradual increase up to three hours. Allowing the samples to depolymerize overnight resulted in a slightly greater increase in G-actin. Comparison of Fig. 1, *a* and *b* indicates that decreases in F-actin were accompanied by corresponding increases in G-actin suggesting that the decrease in TRITC-phalloidin staining does reflect F-actin depolymerization.

The actin present in the high speed pellets at various times after lysis in 0.6 M KCl and 10 μM DNase was also quantified by scanning the actin band on Coomassie blue-stained SDS gels. Gel scans showed 64, 45, and 34% of the initial actin band present 1, 5, and 60 min after lysis of stimulated cells in buffer containing 0.6 M KCl. A TRITC-phalloidin pelleting assay of parallel tubes showed 68, 43, and 29% of the initial values present at these times. Thus, the depolymerization time course followed by SDS gel analysis also correlated well with the time course followed by loss in TRITC-phalloidin staining.

Cytochalasin D Has Similar Effects on the Depolymerization Kinetics of Cellular F-actin and Free Actin Filaments

To predict the filament length distribution from a depolymerization time course, the depolymerization kinetics must be limited by the monomer dissociation rate and not by the dissociation rate of accessory factors that bind to the filament and inhibit depolymerization. To test whether this was the case for the cell actin, we compared the depolymerization kinetics of cell actin with those of pure F-actin in the presence and absence of cytochalasin D (CD). Because CD inhibits depolymerization selectively from the barbed end, the depo-

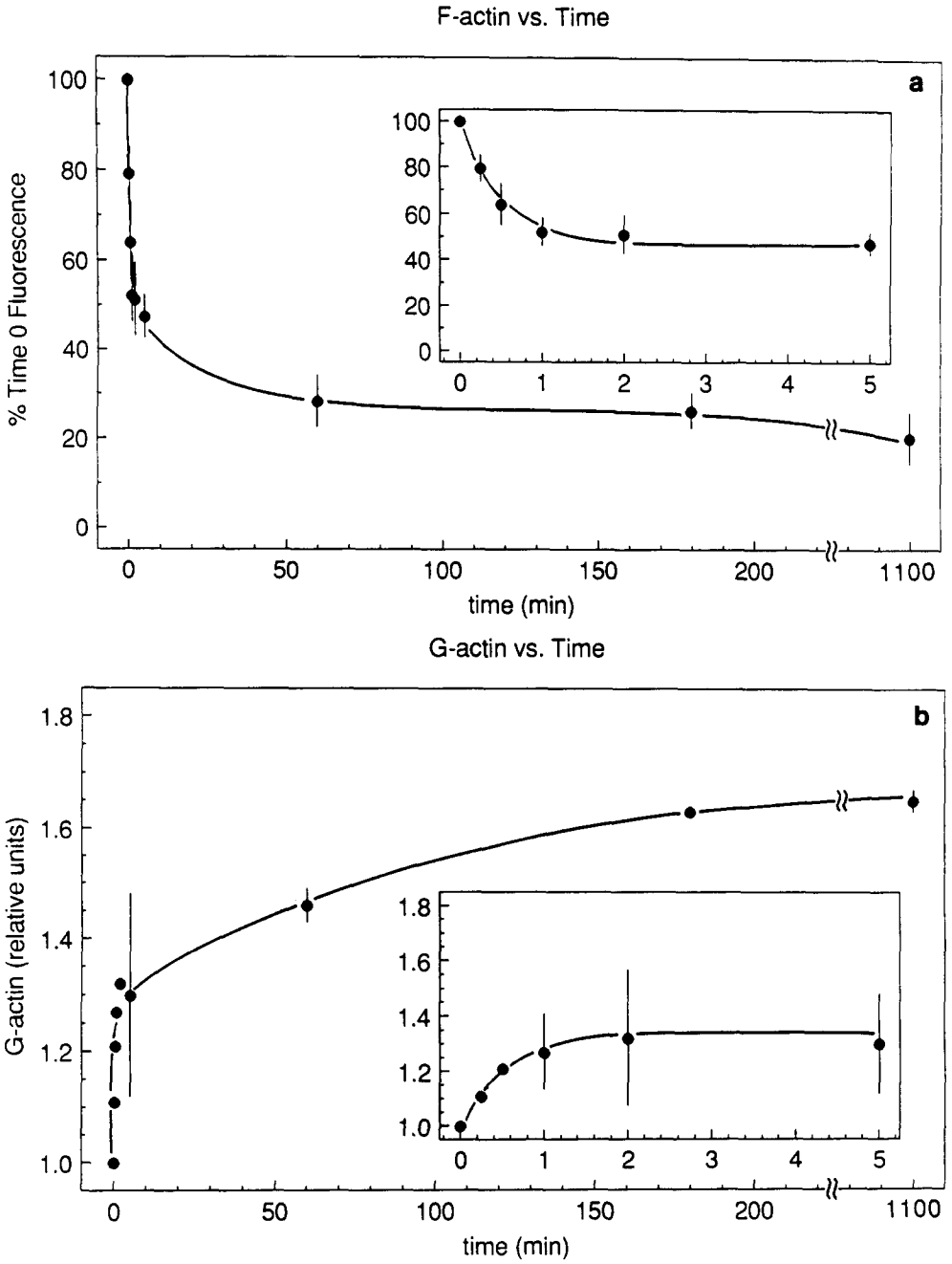

Figure 1. Cell F-actin depolymerization time course by F-actin quantitation or G-actin quantitation. (*a*) Cell actin depolymerization time course for unstimulated cells (2×10^6 cells/ml) lysed in buffer containing 0.6 M KCl and 10 μM DNase I. Data (mean of four experiments ± SEM) are plotted as percent fluorescence relative to the amount of fluorescence at time zero. The inset shows the first five minutes of the time course. (*b*) A DNase inhibition assay (see Materials and Methods) was used to quantify increases in G-actin over the depolymerization time course for unstimulated cells (6×10^5 cells/ml) lysed in buffer containing 0.6 M KCl. Data (mean ± SEM of two experiments) are plotted relative to the amount of inhibition (G-actin) present in the cell lysates at time zero. The inset shows the first five minutes of the time course.

lymerization time course of pure F-actin in the presence of CD is due primarily to depolymerization from the pointed ends of filaments, while the depolymerization time course in the absence of CD is a result of depolymerization from both the barbed and pointed ends of filaments.

For pure actin, free at both ends ($N_b = N_p = N$), the ratio of the depolymerization rates with and without CD is a constant independent of filament number:

$$\frac{\frac{dF}{dt}\ (\text{with CD})}{\frac{dF}{dt}\ (\text{without CD})} \approx \frac{k_{off,p}\ N}{(k_{off,b} + k_{off,p})\ N} = \frac{k_{off,p}}{k_{off,b} + k_{off,p}} \qquad (3)$$

A comparison of this ratio for pure F-actin and for cell F-actin would indicate whether the cell F-actin had equal numbers of free barbed and pointed ends. In contrast, this ratio would increase if some of the barbed ends of the cell F-actin were capped. An increase would also occur if the rate of depolymerization were slowed by some accessory protein, (if the slowing by the accessory factor were minor, its effect would be most apparent on the barbed end kinetics and would increase the ratio; if the accessory factor so slowed the rate that depolymerization was then limited by the off rate of the factor itself, the ratio would be increased to one). The ratio would be decreased only by accessory factors that selectively blocked the pointed end (so far no such factors have been convincingly described) or that increased the depolymerization rate at the barbed end over that of free actin (the opposite of our in vitro results). The fact that CD may

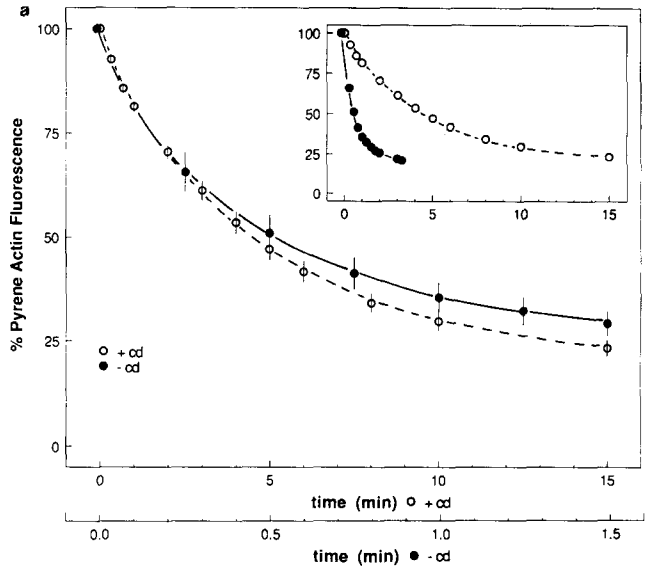

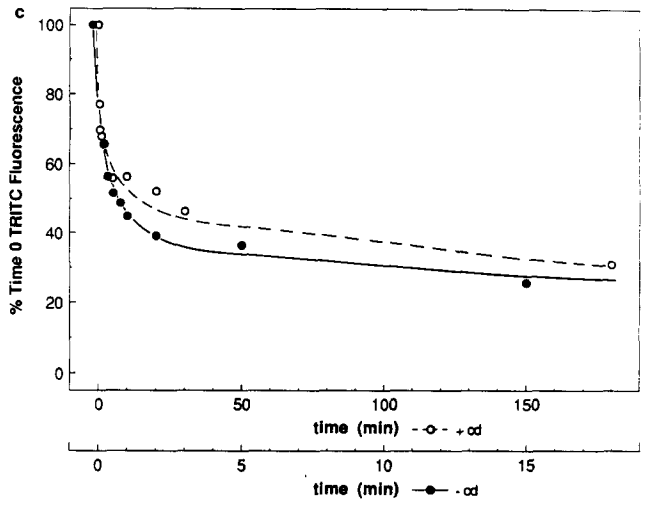

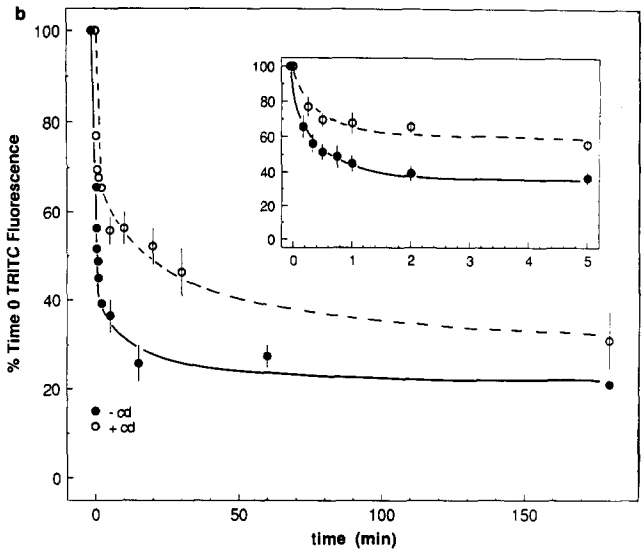

Figure 2. Depolymerization time course of pyrene F-actin and of the F-actin from unstimulated cells in the presence and absence of cytochalasin D. (*a*) Time course of pyrene actin depolymerization in the presence or absence of 0.2 μM CD with time scales that differ by a factor of 10. This scale factor was chosen such that the depolymerization time courses with and without CD would superimpose. 50 μl of 2.0 μM polymerized pyrene-labeled muscle actin was diluted into 1 ml lysis buffer containing 1.2 M KCl and 10 μM DNase I in the presence or absence of 0.2 μM CD. The time courses of depolymerization were followed by decreases in fluorescence (ex 370, em 410). Data (mean ± SEM of three experiments with the same F-actin) are plotted as percent fluorescence relative to the amount of fluorescence present at time zero. Inset shows both time courses plotted with the same time scale. (*b*) Time course of cell F-actin depolymerization for unstimulated cells (2×10^6 cells/ml) lysed in buffer containing 1.2 M KCl and 10 μM DNase I in the presence or absence of 0.2 μM CD. At various times after lysis, 0.6 μM TRITC-phalloidin was added to stop the depolymerization. Data (mean ± SEM of four experiments) are plotted as percent fluorescence relative to the amount of fluorescence present at time zero. The inset shows the first five minutes of the time course. (*c*) Time course of cell F-actin depolymerization for unstimulated cells in the presence or absence of 0.2 μM CD plotted with time scales that differ by a factor of 10. The data of *b* is replotted with different time scales to determine the proportion of cellular F-actin that depolymerized with kinetics similar to pure pyrene-labeled muscle actin (see text for explanation).

not completely block barbed ends (Bonder and Mooseker, 1986) does not interfere with this analysis because the effects of CD should be similar on the pure actin standard and cell actin.

The depolymerization of pyrene F-actin was followed under our conditions (1.2 M KCl and 10 μM DNase) in the presence and absence of 0.2 μM CD. The depolymerization time course of this pyrene-labeled pure muscle actin had the same shape in the presence or absence of 0.2 μM CD, but the ratio of depolymerization rates was ~1/10 (Fig. 2 *a*).

Fig. 2 *b* shows the cell F-actin depolymerization time courses for control cells lysed in 1.2 M KCl and 10 μM DNase I in the presence and absence of 0.2 μM CD. CD slows the time course of depolymerization suggesting that in the absence of CD the cell F-actin is depolymerizing from both barbed and pointed ends. If the data of Fig. 2 *b* is replotted with two time scales that differ by a factor of 10 (Fig. 2 *c*), the cell actin depolymerization time courses in the presence and absence of CD also have a similar shape over the time required for ~70% of the F-actin to depolymerize. Quantitatively similar results were obtained when chemoattractant stimulated cells were lysed in the presence and absence of CD (not shown). These observations suggest that under these lysis conditions, about 70% of the F-actin from stimulated and control cells depolymerizes as free actin filaments. The remaining 30% depolymerizes very slowly, the

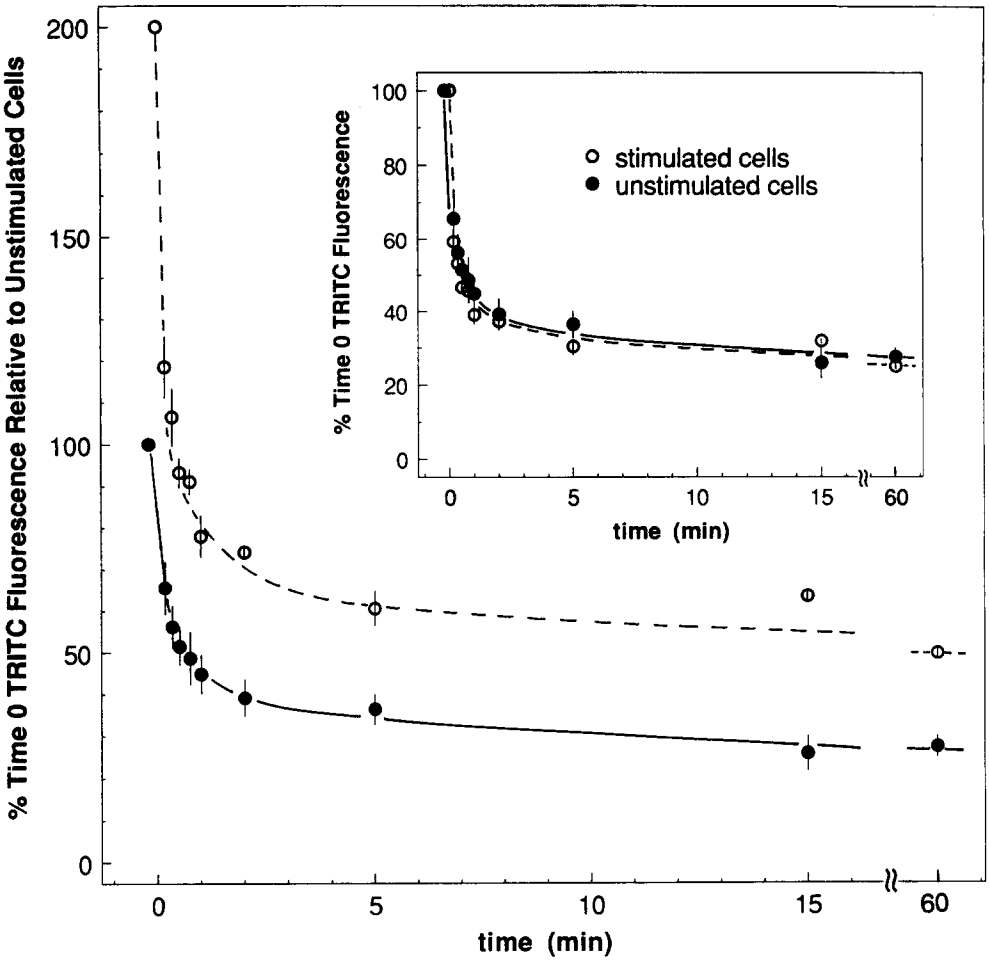

Figure 3. Cell actin depolymerization time courses by F-actin quantitation. Time courses of stimulated and unstimulated cell actin depolymerization in lysates. Cells were incubated at room temperature for 90 s in cell buffer with or without 0.02 μM fNLLP and then lysed at 2 $\times$ 10^6 cells/ml in buffer containing 1.2 M KCl and 10 μM DNase I. At various times after lysis, 0.6 μM TRITC-phalloidin was added to stop the depolymerization. Samples were then processed as described in Materials and Methods for quantitation of F-actin. The data (mean $\pm$ SEM of four experiments) are plotted as percent fluorescence remaining relative to the amount of fluorescence in unstimulated cells at time zero. (*Inset*) Normalized time courses of stimulated and unstimulated cell actin depolymerization in lysates. Data are normalized to 100% F-actin present at time 0 in each case (i.e., relative to the amount of F-actin in each case).

rate similar with or without CD, and therefore must be hindered from depolymerization by accessory factors present in the cell (see Discussion).

Cell F-actin Depolymerization Curves for Control and Chemoattractant Stimulated Cells

Fig. 3 shows the depolymerization time courses for the cell actin in lysates (1.2 M KCl and 10 μM DNase I) from control cells and from cells stimulated at room temperature with 0.02 μM fNLLP for 90 s before lysis. The data are plotted as percent TRITC-phalloidin staining relative to the TRITC-phalloidin staining of control cells at time zero. On the average, stimulation caused a twofold increase in the amount of F-actin when compared to resting cells in the same experiment. Stimulation also resulted in an increase in the initial rate of depolymerization. In stimulated cells there was an increase in the amount of F-actin that rapidly depolymerized as well as an increase in the amount of actin that did not depolymerize even after 60 min under these lysis conditions. For both control and stimulated lysates, there was a rapid initial rate of depolymerization that slowed significantly after 2 to 5 min.

The inset of Fig. 3 shows the F-actin depolymerization time course for stimulated and control cells each normalized to the amount of F-actin at the time of lysis. In both cases, ~70% of the F-actin depolymerized in 15 min. These normalized time courses show the similar shape of the two curves with the curve for stimulated cells falling slightly faster.

Analysis of the Cellular F-actin Depolymerization Time Courses

If we assume that the number of free barbed ends equals the number of free pointed ends ($N_b = N_p = N$) we can approximate Eq. 2 as a difference equation:

$$\frac{\Delta F}{\Delta t} = -(k_{off,b} + k_{off,p})N \qquad (4)$$

As shown above, comparison of the depolymerization time courses in the presence and absence of CD suggested that this is the case during the time required for the first 70% of the cell F-actin to depolymerize. From the slopes of the depolymerization time courses (in units of monomers/s) and the dissociation rate constants measured under our experimental conditions, it is possible to calculate the number of filaments, N, depolymerizing. To evaluate the slope, the fluorescence data must be converted to the amount of actin in filaments. There is ~0.13 nmole of actin in 10^6 cells; between 30 and 50% of this actin in a resting cell is F-actin (White et al., 1983). Assuming 40% of the actin in resting cells is F-actin, we estimated that the fluorescence at time zero for control cells (100% on the figures) is due to 3.1 $\times$ 10^7 actin molecules/cell in filaments. The twofold increase upon stimulation means that the fluorescence at time zero of

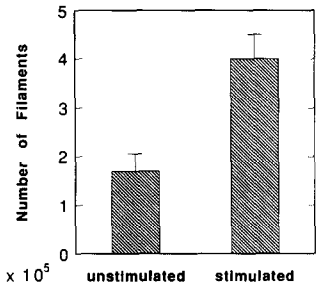

Figure 4. Stimulation results in an increase in the total number of actin filaments. The initial slopes of Fig. 3 were used to calculate the number of actin filaments depolymerizing from stimulated and unstimulated cells. Filament number was calculated using equation (4) and $(k_{off,b} + k_{off,p}) = 6.3\ s^{-1}$. Data are plotted as a mean ± SEM of four experiments.

stimulated cells is due to 6.2×10^7 actin molecules/cell in filaments. The dissociation rate constant for the barbed and pointed ends depolymerizing together in our lysis buffer, $(k_{off,b} + k_{off,p})$, was estimated to be $6.3\ s^{-1}$ (see Materials and Methods).

The initial slope of the depolymerization time course is proportional to the number of actin filaments exhibiting depolymerization at the time of lysis. Chemoattractant stimulation resulted in a faster initial rate of depolymerization and thus an increase in the number of actin filaments exhibiting depolymerization. The initial rate of depolymerization of stimulated cells was also faster than control cells when assayed in lysis buffer containing 0.2 μM CD indicating an increase in the number of pointed ends. From the initial slopes of Fig. 3 and the rate constant described above, we estimated that resting PMNs had $1.7 \pm 0.4 \times 10^5$ filaments/cell while stimulation with chemoattractant for 90 s increased the initial rate by 2.4× and thus, increased the filament number to $4.0 \pm 0.5 \times 10^5$ filaments/cell (Fig. 4).

To analyze the data for a filament length distribution, the depolymerization time courses were approximated by a series of straight lines using least squares analysis (Fig. 5, *inset*). We included the maximum number of points per line segment such that the correlation coefficient for each segment was ≥0.9. By applying Eq. 4, we calculated filament number as a function of time. The change in rate represented a loss of filaments because of complete depolymerization, thus the length of the filaments lost is defined by the dissociation rate constant multiplied by the time it took for them to depolymerize. Fig. 5 shows the calculated filament distribu-

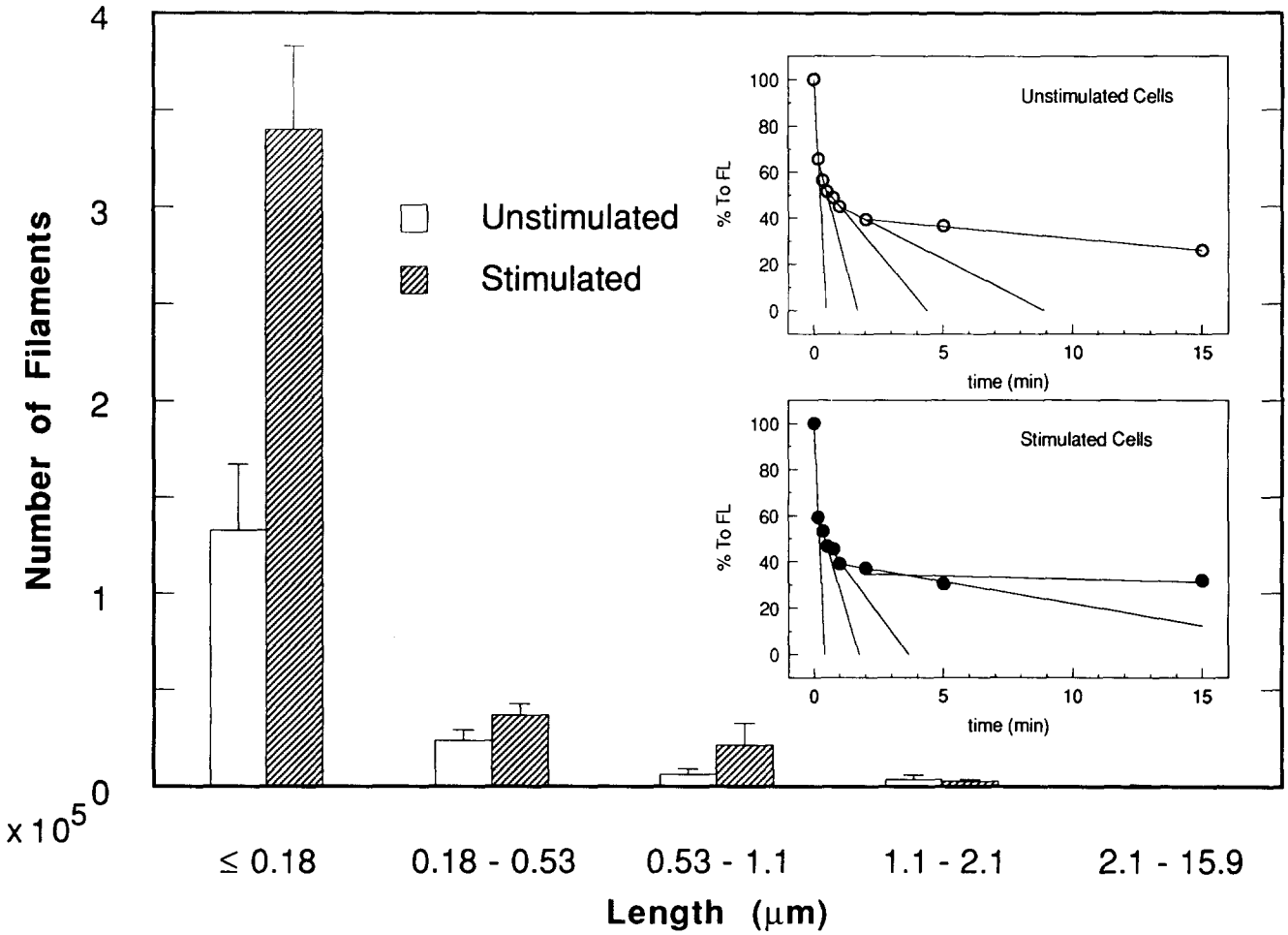

Figure 5. Approximate actin filament length distribution for depolymerizable actin in stimulated and unstimulated cells. Analysis of the depolymerization time courses (Fig. 3) using $(k_{off,b} + k_{off,p}) = 6.3\ s^{-1}$ resulted in five discrete length populations (see text). Solid bars are filament numbers for unstimulated cells while hatched bars are filament numbers for stimulated cells. Data are mean ± SEM of four experiments. Insets show the line segments used to approximate the cell actin depolymerization curves given by the means of the data to obtain the mean discreet filament length distribution.

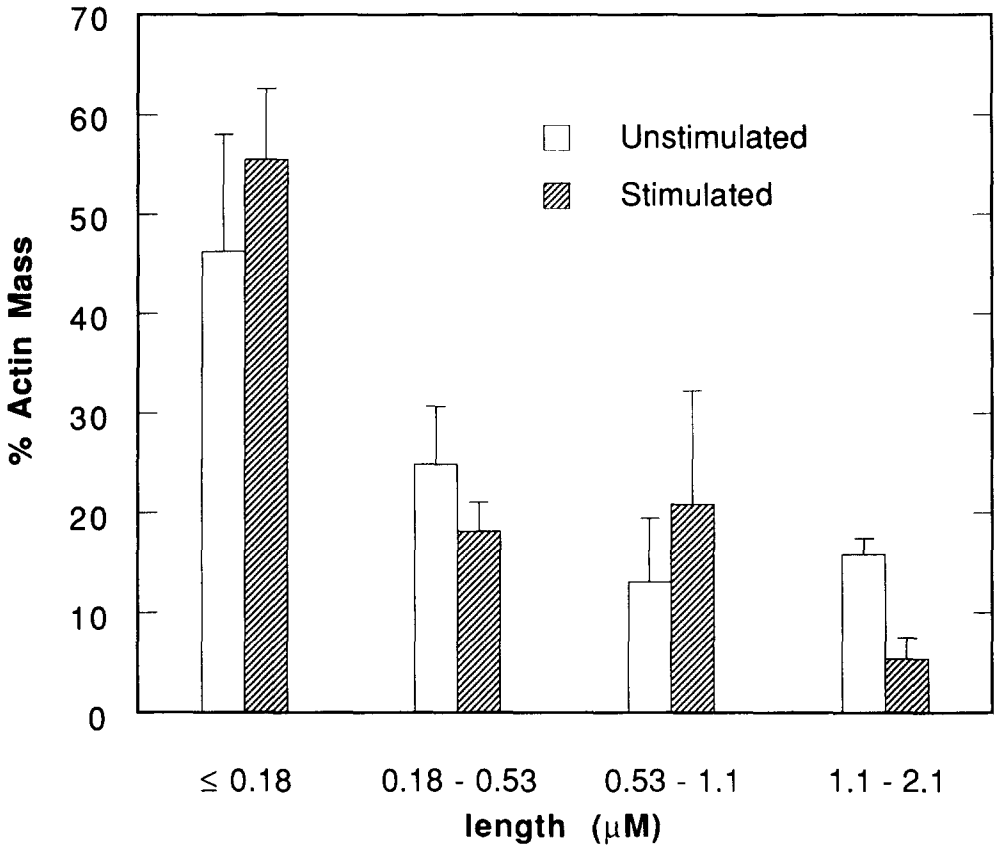

Figure 6. Actin mass distribution for depolymerizable actin in stimulated and unstimulated cells. The data of Fig. 5 were used to calculate a distribution of the percent actin mass found in each of the first four discrete filament length populations.

tion for the depolymerizable F-actin (~70% of total) in stimulated and control cells. The distributions are very similar. In both cases ~80% of the filaments appear to be quite short (≤0.18 μm). The average filament length for control cells is 0.29 ± 0.09 μm and the average for stimulated cells is 0.27 ± 0.07 μm. The fifth (longest) length population was not included in the average length calculation because it reflects interference from the pool that does not depolymerize. Fig. 6 is a plot of the actin mass distribution in the first four length classes that were defined in Fig. 5. Most of the actin mass is found in the short filaments.

This analysis of depolymerization time courses in terms of filament length distributions assumes that the slowing of the time course is because of the progressive loss of filaments. To verify this assumption, we examined the loss of elongation sites for actin polymerization (presumably barbed ends of filaments since addition of CD completely inhibited elongation) during the depolymerization time course. 2.0 μM pyrene-labeled G-actin was added to lysates at various times during the depolymerization time course. The initial increase in fluorescence (i.e., the initial rate of polymerization) was taken to be proportional to the number of actin elongation sites present. From the initial rates of polymerization due to control or stimulated cells lysed into buffer containing 0.6 M KCl and 2.0 μM pyrene-labeled G-actin, we estimated that there were 1.7×10^5 elongation sites/control cell and 2.7×10^5 elongation sites/stimulated cell. Fig. 7 shows the loss of actin elongation sites during depolymerization of the actin from control cells in lysis buffer containing 0.6 M KCl (turbidity of the samples made it impossible to perform this assay in 1.2 M KCl). Similar results were obtained for stimulated cells (not shown). The loss in elongation sites occurs over the same time course as the decrease in filament number from the depolymerization data thus supporting the assumption that the depolymerization time course reflects a progressive loss of actin filaments.

Discussion

Previous studies have shown that chemoattractant stimulation causes a twofold increase in the F-actin content of PMNs. We have now used a kinetic analysis to show that a twofold increase in the number of actin filaments accompanies the twofold increase in F-actin. The rate of F-actin depolymerization in both the presence and absence of CD was faster in stimulated than unstimulated cells. This observation only rules out the possibility that the chemoattractant-induced increase in F-actin is merely a result of the removal of barbed end-capping proteins and subsequent elongation from these new ends. We estimated that resting cells had about $1.7 \pm 0.4 \times 10^5$ filaments with average length 0.29 ± 0.09 μm while stimulated cells had $4.0 \pm 0.5 \times 10^5$ filaments with average length 0.27 ± 0.07 μm. Most (~80%) of the filaments in both stimulated and control cells were quite short (~0.18 μm). The shape of the filament length distribution was similar in stimulated and control cells.

An increase in the filament number of chemoattractant stimulated cells is consistent with earlier observations that chemoattractant stimulation increased the number of actin elongation sites in cell lysates (Carson et al., 1986; Howard et al., 1990). Carson et al. (working at 37°C) showed that elongation sites doubled upon stimulation with chemoattrac-

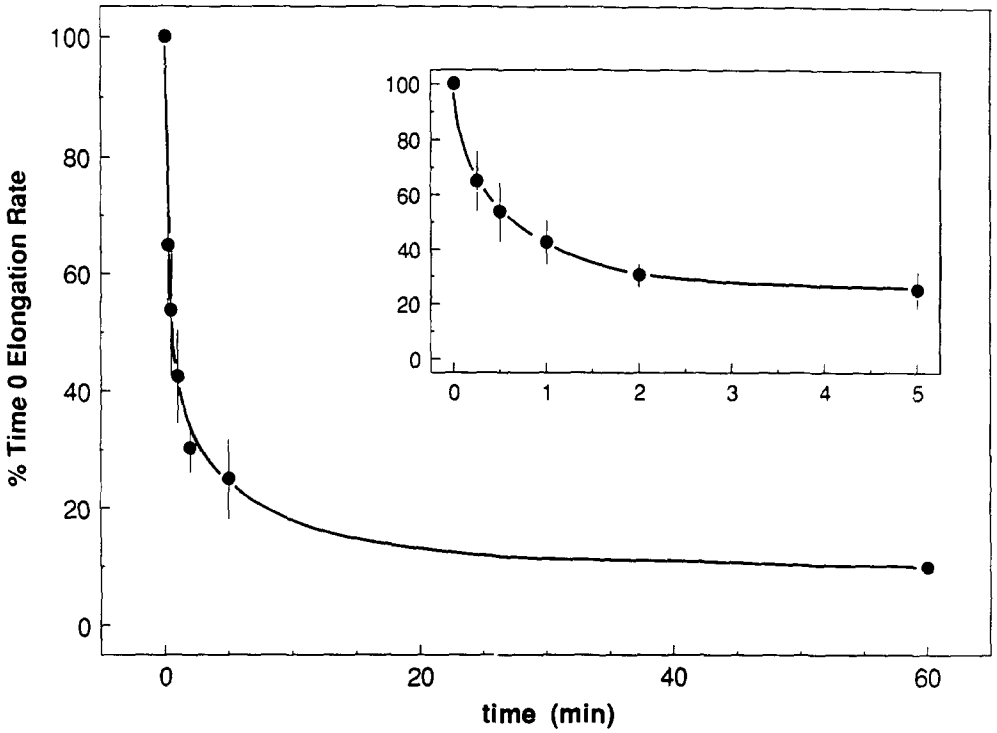

Figure 7. Loss of elongation sites for exogenous actin polymerization during the depolymerization time course. Lysates were prepared from unstimulated cells at 10^6 cells/ml in lysis buffer containing 0.6 M KCl; at various times, 2.0 μM pyrene G-actin was added to the mixture. The initial increase in fluorescence was taken to be proportional to changes in the number of actin elongation sites present. Data (mean ± SEM of two experiments) are plotted as percent elongation rate relative to the elongation rate found by lysing cells directly into buffer containing 2.0 μM pyrene G-actin.

tant, peaking at ~10 s and then declining. In the current study (working at room temperature), we find about a 1.6-fold increase in elongation sites after 90 s. This difference is due in part to the different temperatures of the experiments; at 37°C the elongation activity and the F-actin level rise and decline rapidly while at room temperature both rise and fall more slowly. Since the elongation sites could have arisen from the cutting or uncapping of existing filaments or from de novo sites, we could not predict from the earlier study (Carson et al., 1986) whether filament number or length, or both, were increased by addition of chemoattractant. The increase in filament number suggested by our kinetic data could be explained by severing of existing filaments or by creation of new filaments from de novo nucleation sites. The simple removal of a capping protein from existing filaments would not lead to an increase in filament number. However, the new elongation sites could result from the uncapping of small actin oligomers that are too small to pellet and thus be counted as filaments. Small oligomers are reported to be released from gelsolin–actin complexes upon chemoattractant stimulation (Howard et al., 1990).

To interpret the depolymerization time course of cellular F-actin in terms of a filament length distribution, it is critical to know if the depolymerization of cellular F-actin is limited by the actin dissociation constants under the conditions of the assays. To eliminate effects of G-actin on the kinetics (as in Eq. 2) we included 10 μM DNase I to bind actin monomers. This was preferable to dilution of samples to decrease G-actin concentration since after extensive dilution, the data became very noisy (presumably from adsorption of TRITC-phalloidin to the large surface area of the tubes). While DNase I binds to the pointed ends of filaments (Podolski and Steck, 1990), it does not inhibit depolymerization from the pointed end (Annemarie Weber, University of Pennsylvania, Philadelphia, PA personal communication). By comparing the effect of DNase I on long and short actin filaments, Dr. Weber has shown that DNase I increases the rate of depolymerization from the pointed end of the filament by increasing the dissociation rate constant and not by severing the filaments. We confirmed these results in our laboratory. In the presence of protease inhibitors, we saw that 10 μM DNase I slightly increased (~1.5×) the rate of pyrene actin depolymerization. Since both control and stimulated lysates were treated similarly, the relative change in filament number upon stimulation is not affected by the particular rate constant used.

In 1.2 M KCl and 10 μM DNase I, ~70% of the F-actin depolymerized in 5 min (Fig. 3). The kinetics with and without cytochalasin D (Fig. 2) suggest that this actin depolymerized similarly to free filaments, i.e., not limited by other factors such as cross-linking or capping proteins. The high KCl probably helps remove salt-sensitive actin-binding proteins that inhibit the rate and extent of depolymerization. For example, acumentin, tropomyosin, and actin-binding protein dissociate from actin in the presence of high salt (Southwick and Stossel, 1981; Southwick et al., 1982; Maekawa et al., 1989; Broschat and Burgess, 1986; Rosenburg et al., 1981).

Changes in the slope of the depolymerization time course (Fig. 3) could be due to losses of entire filaments via depolymerization (Fig. 8 *B*) or to filaments whose depolymerization becomes blocked by associated factors (Fig. 8 *A*). The loss of elongation sites over the time course of depolymerization (Fig. 7) suggests that filament ends are disappearing as the actin depolymerizes. The depolymerization time course data suggest that 90% of the filaments disappear after 5 min while the elongation experiments suggest that only 70% of the filaments disappear after 5 min. This difference is not due to the fact that the elongation experiments were performed in 0.6 M KCl while the depolymerization experiments were

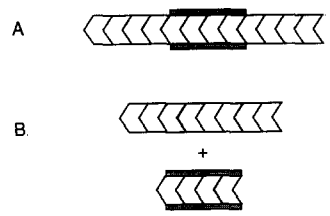

Figure 8. Schematic representation of possible models of the F-actin in polymorphonuclear leukocytes. Cellular F-actin may be in one of two simple forms. (*A*) Actin filaments may be partially associated with factors (▨) that can block depolymerization. Under our lysis conditions, the F-actin would depolymerize until a block was reached. (*B*) Or there may be two classes of actin filaments. Under our lysis conditions one class would completely depolymerize, while the other class would not depolymerize because it is blocked by filament associated factors (▨).

performed in 1.2 M KCl since analysis of depolymerization kinetics in 0.6 M KCl also shows a loss of ~90% of the filaments in 5 min (unpublished data). The residual 20% of the elongation activity is probably due to free ends of filaments present in the 30% of the F-actin that does not depolymerize.

Our filament numbers and lengths are estimated from the 70% of the F-actin that has depolymerized in 5 min. The residual 30% of the actin could affect the estimated filament length distribution. One possibility, suggested above, is that our calculated distribution accounts for depolymerizable ends of filaments that are inhibited from complete depolymerization (Fig. 8 *A*). Were this the case, we would have correctly estimated the filament number but underestimated filament length by ~30%. It is also possible that the residual 30% of the F-actin in 1.2 M KCl represents additional separate filaments (Fig. 8 *B*). Were this the case we would have underestimated the filament number by about 20% (the residual elongation sites). Since 20% of the elongation sites remain while 30% of the total F-actin remains, this residual F-actin would be expected to have a similar, but slightly longer filament length distribution, than the rest of the filaments.

Our analysis reduced the filament distribution to five discrete filament length classes. The true filament length distribution is likely to be continuous. A nonlinear least squares routine was used to fit some continuous functions (for example, a sum of exponentials or a sum of error functions) to the depolymerization data (not shown). By taking the first derivative of these functions, we were able to obtain smooth curves that would represent the number of filaments versus time. The rate of change of these curves was then used to calculate continuous distributions. We found the predicted continuous length distributions were quite sensitive to the function chosen for curve fitting, especially in the small filament range. However, curve fitting interpolated our data beyond its resolution, especially at short times where we were unable to distinguish which fit was better and there was no compelling reason why either should be applied. If filaments were pooled into discrete classes we obtained the same general result as the division of F-actin into discrete length populations (many small filaments, some intermediate filaments, and few long filaments both in stimulated and control cells). Therefore, we have chosen to report our results in terms of discrete length populations.

Our data suggest that there are a very large number of short filaments present within stimulated and unstimulated PMNs. It is not possible to measure filament lengths in electron micrographs of PMNs (Ryder et al., 1984) because of the difficulty in resolving free filament ends (i.e., do filaments cross over or terminate at the intersections). Similar actin meshworks have been observed in macrophages and *Dictyostelium discoideum* (Hartwig and Shevlin, 1986; Hartwig and Yin, 1988; Rubino and Small, 1987). Hartwig and Shevlin (1986) measured the distance between filament intersections in macrophages (~0.1 μm) but also were unable to morphometrically measure the end-to-end length of individual filaments. In *D. discoideum* the majority of filaments measured morphologically were approximately 0.1-μm long (Rubino and Small, 1987). All of the electron microscopic observations are compatible with our estimates of the filament lengths from kinetic data.

The time course of the F-actin depolymerization in lysates has been used to estimate the actin filament length distribution of unstimulated *D. discoideum* (Podolski and Steck, 1990). The data suggested about 3.6×10^5 filaments/*Dictyostelium* with an average length of 0.2 μm and the existence of a very large population of small filaments (0.14 μm). In that analysis, it was not clear whether 100% of the F-actin depolymerized; nor was there any evidence showing the depolymerization kinetics were not affected by filament associated factors. Nevertheless, the filament number and distribution obtained for unstimulated *Dictyostelium* amoeba were similar to ours for unstimulated PMNs.

In summary, stimulation with chemoattractant appears to increase F-actin levels in PMNs by increasing the filament number while keeping the filament length distribution quite constant. The fact that the filament length distribution does not change upon stimulation suggests that this distribution is similar in the lamellipodia and the cortex since most of the F-actin induced by chemoattractant is in the lamellipodia. Thus the increased lability of lamellar F-actin relative to cortical F-actin that has been observed in vivo (Cassimeris et al., 1990) is not likely to be because of a difference in the filament lengths. The functional significance and molecular basis for creating the filament length distribution requires further study.

We thank Lynne Cassimeris for running the SDS gels, critically reading the manuscript, and for helpful discussions, Michael Joyce for excellent technical assistance, Mark Mooseker for providing us with villin, and Annemarie Weber, Martin Pring, Vivianne Nachmias, and Marc Symons for critically reading the manuscript.

This work was supported by National Institutes of Health grant Al 19883 to S. H. Zigmond, National Institutes of Health grant GM 41476 to D. A. Lauffenburger, and a National Science Foundation predoctoral fellowship to M. L. Cano.

Received for publication 17 April 1991 and in revised form 16 July 1991.

References

Blikstad, I., F. Markey, L. Carlsson, T. Persson, and U. Lindberg. 1978. Selective assay for monomeric and filamentous actin in cell extracts, using inhibition of deoxyribonuclease I. *Cell.* 15:935-943.

Bonder, E. M., and M. S. Mooseker. 1986. Cytochalasin B slows but does not prevent monomer addition at the barbed end of the actin filament. *J. Cell Biol.* 102:282-288.

Broschat, K. O. 1990. Tropomyosin prevents depolymerization of actin filaments from the pointed end. *J. Biol. Chem.* 265:21323-21329.

Broschat, K. O., A. Weber, and D. R. Burgess. 1989. Tropomyosin stabilizes the pointed end of actin filaments by slowing depolymerization. *Biochemistry.* 28:8501-8506.

Broschat, K. O., and D. R. Burgess. 1986. Low M_r tropomyosin isoforms from chicken brain and intestinal epithelium have distinct actin-binding properties. *J. Biol. Chem.* 261:13350-13359.

Carson, M., A. Weber, and S. H. Zigmond. 1986. An actin-nucleating activity in polymorphonuclear leukocytes is modulated by chemotactic peptides. *J. Cell Biol.* 103:2707–2714.

Cassimeris, L., H. McNeill, and S. H. Zigmond. 1990. Chemoattractant-stimulated polymorphonuclear leukocytes contain two populations of actin filaments that differ in their spatial distributions and relative stabilities. *J. Cell Biol.* 110:1067–1075.

Cooper, J. A. 1987. Effects of cytochalasins and phalloidin on actin. *J. Cell Biol.* 105:1473–1478.

Fechheimer, M., and S. H. Zigmond. 1983. Changes in cytoskeletal proteins of polymorphonuclear leukocytes induced by chemotactic peptides. *Cell Motil.* 3:349–361.

Grazi, E., and G. Trombetta. 1986. Evaluation of the actin filament length from the time course of the depolymerization process. *Biochem. Biophys. Res. Commun.* 139:109–114.

Hartwig, J. H., and H. L. Yin. 1988. The organization and regulation of the macrophage actin skeleton. *Cell Motil. & Cytoskel.* 10:117–125.

Hartwig, J. H., and P. Shevlin. 1986. The architecture of actin filaments and the ultrastructural location of actin-binding protein in the periphery of lung macrophages. *J. Cell Biol.* 103:1007–1020.

Howard, T. H., and C. O. Oresajo. 1985*a*. The kinetics of chemotactic peptide-induced change in F-actin content, F-actin distribution, and the shape of neutrophils. *J. Cell Biol.* 101:1078–1085.

Howard, T. H., and C. O. Oresajo. 1985*b*. A method for quantifying F-actin in chemotactic peptide activated neutrophils: study of the effect of fBOC peptide. *Cell Motil.* 5:545–557.

Howard, T. H., C. Chapponier, H. Yin, and T. Stossel. 1990. Gelsolin-actin interaction and actin polymerization in human neutrophils. *J. Cell Biol.* 110: 1983–1991.

Johnson, K. A., and G. G. Borisy. 1977. Kinetic analysis of microtubule self-assembly in vitro. *J. Mol. Biol.* 117:1–31.

Karr, T. L., D. Kristofferson, and D. L. Purich. 1980. Mechanism of microtubule depolymerization. *J. Biol. Chem.* 255:8560–8566.

Kristofferson, D., T. L. Karr, and D. L. Purich. 1980. Dynamics of linear protein polymer disassembly. *J. Biol. Chem.* 255:8567–8572.

Laemmli, U. K. 1970. Cleavage of structural proteins during the assembly of the head of bacteriophage T4. *Nature (Lond.).* 227:680–685.

Lal, A. F., and E. D. Korn. 1986. Effect of muscle tropomyosin on the kinetics of polymerization of muscle actin. *Biochemistry.* 25:1154–1158.

Maekawa, S., M. Toriyama, and H. Sakai. 1989. Tropomyosin in the sea urchin egg cortex. *Eur. J. Biochem.* 178:657–662.

Northrop, J., A. Weber, M. S. Mooseker, C. Franzini-Armstrong, M. F. Bishop, G. R. Dubyak, M. Tucker, and T. P. Walsh. 1986. Different calcium dependence of the capping and cutting activities of villin. *J. Biol. Chem.* 261:9274–9281.

Podolski, J. L., and T. L. Steck. 1990. Length distribution of F-actin in Dictyostelium discoideum. *J. Biol. Chem.* 265:1312–1318.

Rao, K., and J. Varani. 1982. Actin polymerization induced by chemotactic peptide and concanavalin A in rat neutrophils. *J. Immunol.* 129:1605–1607.

Rosenburg, S., A. Stracher, and R. C. Lucas. 1981. Isolation and characterization of actin and actin-binding protein from human platelets. *J. Cell Biol.* 91:201–211.

Rubino, S., and J. V. Small. 1987. The cytoskeleton of spreading Dictyostelium amoebae. *Protoplasma.* 136:63–69.

Ryder, M. I., R. N. Weinreb, and R. Niederman. 1984. The organization of actin filaments in human polymorphonuclear leukocytes. *Anat. Rec.* 209:7–20.

Schliwa, M., and J. VanBlerkom. 1981. Structural interaction of cytoskeletal components. *J. Cell Biol.* 90:222–235.

Southwick, F. S., and T. P. Stossel. 1981. Isolation of an inhibitor of actin polymerization from human polymorphonuclear leukocytes. *J. Biol. Chem.* 256:3030–3036.

Southwick, F. S., N. Tatsumi, and T. P. Stossel. 1982. Acumentin, an actin-modulating protein of rabbit pulmonary macrophages. *Biochemistry.* 21:6321–6326.

Spudich, J. A., and S. Watt. 1971. The regulation of rabbit muscle contraction: biochemical studies of the interaction of the tropomyosin-troponin complex with actin and the proteolytic fragments of myosin. *J. Biol. Chem.* 246:4866–4871.

Wallace, P. J., R. P. Wersto, C. H. Packman, and M. A. Lichtman. 1984. Chemotactic peptide-induced changes in neutrophil actin conformation. *J. Cell Biol.* 99:1060–1065.

Weigt, C., B. Schoepper, and A. Wegner. 1990. Tropomyosin-troponin complex stabilizes the pointed ends of actin filaments against polymerization and depolymerization. *FEBS (Fed. Eur. Biochem. Soc.) Lett.* 260:266–268.

White, J. R., P. H. Naccache, and R. I. Sha'afi. 1983. Stimulation by chemotactic factors of actin association with the cytoskeleton in rabbit neutrophils (role of calcium and cytochalasin B). *J. Biol. Chem.* 258:14041–14047.

Yahara, I., F. Harada, S. Sekita, K. Yoshihira, and S. Natori. 1982. Correlation between effects of 24 different cytochalasins on cellular structures and cellular events and those on actin in vitro. *J. Cell Biol.* 92:69–78.

Zigmond, S. H., and S. J. Sullivan. 1979. Sensory adaptation of leukocytes to chemotactic peptides. *J. Cell Biol.* 82:517–527.